Nonleptonic two-body decays of the B_c meson in the light-front quark model and the QCD factorization approach

Ho-Meoyng Choi[1] and Chueng-Ryong Ji[2]

[1]*Department of Physics, Teachers College, Kyungpook National University, Daegu, Korea 702-701*
[2]*Department of Physics, North Carolina State University, Raleigh, North Carolina 27695-8202, USA*

We study exclusive nonleptonic two-body $B_c \to (D_{(s)}, \eta_c, B_{(s)}) + F$ decays with F (pseudoscalar or vector mesons) factored out in the QCD factorization approach. The nonleptonic decay amplitudes are related to the product of meson decay constants and the form factors for semileptonic B_c decays. As inputs in obtaining the branching ratios for a large set of nonleptonic B_c decays, we use the weak form factors for the semileptonic $B_c \to (D_{(s)}, \eta_c, B_{(s)})$ decays in the whole kinematical region and the unmeasured meson decay constants obtained from our previous light-front quark model. We compare our results for the branching ratios with those of other theoretical studies.

I. INTRODUCTION

The discovery of the B_c meson by the Collider Detector at Fermilab (CDF) Collaboration [1] in $p\bar{p}$ collisions at $\sqrt{s} = 1.8$ TeV and the subsequent measurement of its lifetime have provided a new window for the analysis of the heavy-quark dynamics and thus for an important test of quantum chromodynamics. Recently the CDF and D0 Collaborations announced some new measurements of the B_c meson lifetime and mass [2,3], $\tau_{B_c} = 0.463^{+0.073}_{-0.065}(\text{stat}) \pm 0.036(\text{syst})$ ps [2], $M_{B_c} = 6275.6 \pm 2.9(\text{stat}) \pm 2.5(\text{syst})$ MeV [2], and $6300 \pm 14(\text{stat}) \pm 5(\text{syst})$ MeV [3]. The LHC is expected to produce around $\sim 5 \times 10^{10}$ B_c events per year [4,5]. This will provide more detailed information on the decay properties of the B_c meson. Since the B_c mesons carry flavor explicitly (b and c) and cannot annihilate into gluons, they are stable against strong and electromagnetic annihilation processes. The decays of the B_c meson are therefore only via weak interactions, which can be divided into three classes at the quark level: (1) the $b \to q$ ($q = c, u$) transition with the c quark being a spectator, (2) the $c \to q$ ($q = s, d$) transition with the b quark being a spectator, and (3) the weak annihilation channels. Although the phase space of the $c \to s, d$ transitions is much smaller than the phase space of the $b \to c, u$ transitions, the Cabibbo-Kobayashi-Maskawa (CKM) matrix elements are greatly in favor of the c quark decay, i.e. $|V_{cb}| \ll |V_{cs}|$. In fact, the c-quark decays provide about $\sim 70\%$ of the B_c decay width while the b-quark decays and the weak annihilation yield about 20% and 10%, respectively [5]. This indicates that both b- and c-quark decay processes contribute to the B_c decay width on a comparable footing.

Because the b and c quarks can decay individually and the B_c meson has a sufficiently large mass, one can study a great variety of decay channels. There have been many theoretical efforts to calculate the semileptonic [5–26] and nonleptonic [4–16,27–42] decays of the B_c meson. The

semileptonic B_c decays provide a good opportunity to measure not only the CKM elements such as $|V_{cb}|$, $|V_{ub}|$, $|V_{cs}|$, and $|V_{cd}|$, but also the weak form factors for the transitions of B_c to bottom and charmed mesons. The nonleptonic B_c decays, in which only hadrons appear in the final state, are strongly influenced by the confining color forces among the quarks. While in the semileptonic transitions the long-distance QCD effects are described by a few hadronic form factors parametrizing the hadronic matrix elements of quark currents, the nonleptonic processes are complicated by the phenomenon of the quark rearrangement due to the exchange of soft and hard gluons. The theoretical description of the nonleptonic decays involves the matrix elements of the local four-quark operators. Although the four-quark operators are more complicated than the current operators involved in the semileptonic decays, the nonleptonic decays of the heavy mesons are useful for exploring the most interesting aspect of QCD, i.e. its nonperturbative long-range character.

In our recent paper [43], we analyzed the semileptonic B_c decays such as $B_c \to (D, \eta_c, B, B_s)\ell\nu_\ell$ and $\eta_b \to B_c\ell\nu_\ell(\ell = e, \mu, \tau)$ using our light-front quark model (LFQM) based on the QCD-motivated effective LF Hamiltonian [44–49]. The weak form factors $f_\pm(q^2)$ for the semileptonic decays between two pseudoscalar mesons are obtained in the $q^+ = 0$ frame ($q^2 = -\mathbf{q}_\perp^2 < 0$) and then analytically continued to the timelike region by changing $\mathbf{q}_\perp^2$ to $-q^2$ in the form factor. The covariance (i.e., frame independence) of our model has been checked by performing the LF calculation in the $q^+ = 0$ frame in parallel with the manifestly covariant calculation using the exactly solvable covariant fermion field theory model in $(3 + 1)$ dimensions. We also found the zero-mode contribution to the form factor $f_-(q^2)$ and identified the zero-mode operator that is convoluted with the initial and final state LF wave functions.

In this paper, we extend our previous LFQM analysis of the semileptonic B_c decays [43] to the nonleptonic two-

body decays of B_c mesons such as $B_c \rightarrow (D_{(s)}, \eta_c, B_{(s)})P$ and $B_c \rightarrow (D, \eta_c, B_{(s)})V$ (here P and V denote pseudoscalar and vector mesons, respectively). The QCD factorization approach is widely used since it works reasonably well in heavy-quark physics [50–55]. The factorization approximates the complicated nonleptonic decay amplitude into the product of the meson decay constant and the form factor. A justification of this assumption is usually based on the idea of color transparency [56]. We shall use the form factors for semileptonic $B_c \rightarrow (D_{(s)}, \eta_c, B_{(s)})$ decays as well as the meson decay constants obtained in our LFQM [43,48] as input parameters for the nonleptonic B_c decays. As done by many others [5–14], we consider only the contribution of current-current operators at the tree level and calculate the decay widths for various nonleptonic B_c decays. As far as the decay width is concerned, the contribution from the tree diagram is much larger than that from the penguin diagram. The penguin contribution may be important in evaluating the CP violation and looking for new physics beyond the standard model, which we do not consider in this work.

The paper is organized as follows. In Sec. II, we discuss the weak Hamiltonian responsible for the nonleptonic two-body decays of the B_c meson. In Sec. III, we present the input parameters such as the weak decay constants and the form factors obtained in our LFQM [43,48] based on the QCD-motivated effective Hamiltonian [44,45]. The mixing angles between η and η' mesons are also analyzed, both in octet-singlet and quark-flavor bases, to extract the decay constants relevant to η and η' mesons. Section IV is devoted to the numerical results. A summary and conclusions follow in Sec. V.

II. NONLEPTONIC TWO-BODY DECAYS OF THE B_c MESON

The nonleptonic weak decays are described in the standard model by a single W-boson exchange diagram at tree level. In the standard model, the nonleptonic B_c decays are described by the effective Hamiltonian, which was obtained by integrating out the heavy W boson and top quark. For the case of $b \rightarrow c, u$ and $c \rightarrow s, d$ transitions at the quark level, neglecting QCD penguin operators, one gets the following effective weak Hamiltonian:

$$\mathcal{H}_{\text{eff}}^{b \rightarrow c(u)} = \frac{G_F}{\sqrt{2}} \{ V_{cb}[c_1(\mu)\mathcal{O}_1^{cb} + c_2(\mu)\mathcal{O}_2^{cb}]$$
$$+ V_{ub}[c_1(\mu)\mathcal{O}_1^{ub} + c_2(\mu)\mathcal{O}_2^{ub}] + \text{H.c.} \} \quad (1)$$

and

$$\mathcal{H}_{\text{eff}}^{c \rightarrow s(d)} = \frac{G_F}{\sqrt{2}} \{ V_{cd}[c_1(\mu)\mathcal{O}_1^{cd} + c_2(\mu)\mathcal{O}_2^{cd}]$$
$$+ V_{cs}[c_1(\mu)\mathcal{O}_1^{cs} + c_2(\mu)\mathcal{O}_2^{cs}] + \text{H.c.} \}, \quad (2)$$

where G_F is the Fermi coupling constant and $V_{q_1 q_2}$ are the

TABLE I. Values for CKM matrix elements used in this work.

V_{ud}	V_{us}	V_{cd}	V_{cs}	V_{cb}	V_{ub}
0.974	0.2255	-0.230	1.04	0.0412	0.003 93

corresponding CKM matrix elements. We use the central values of the CKM matrix elements quoted by the Particle Data Group (PDG) [57] that we summarize in Table I. The effective weak Hamiltonian consists of products of local four-quark operators $\mathcal{O}_{1,2}$ renormalized at the scale μ, and scale-dependent Wilson coefficients $c_{1,2}(\mu)$, which incorporate the short-distance effects arising from the renormalization of $\mathcal{H}_{\text{eff}}$ from $\mu = m_W$ to $\mu = O(m_b)$. The local four-quark operators $\mathcal{O}_1$ and $\mathcal{O}_2$ due to b and c decays are given by

$$\mathcal{O}_1^{qb} = (\bar{q}b)_{V-A}[(\bar{d}'u)_{V-A} + (\bar{s}'c)_{V-A}](q = c, u),$$
$$\mathcal{O}_2^{qb} = (\bar{q}u)_{V-A}(\bar{d}'b)_{V-A} + (\bar{q}c)_{V-A}(\bar{s}'b)_{V-A}(q = c, u),$$
$$\mathcal{O}_1^{cq} = (\bar{c}q)_{V-A}(\bar{d}'u)_{V-A}(q = s, d),$$
$$\mathcal{O}_2^{cq} = (\bar{c}u)_{V-A}(\bar{d}'q)_{V-A}(q = s, d), \quad (3)$$

where $(\bar{q}q)_{V-A} = \bar{q}\gamma_\mu(1 - \gamma_5)q$ and the rotated antiquark fields are given by

$$\bar{d}' = V_{ud}\bar{d} + V_{us}\bar{s}, \qquad \bar{s}' = V_{cd}\bar{d} + V_{cs}\bar{s}. \quad (4)$$

Without strong-interaction effects, one would have $c_1 = 1$ and $c_2 = 0$. However, this simple result is modified by gluon exchange: i.e., the original weak vertices get renormalized and the new types of interactions (such as the operators $\mathcal{O}_2$) are induced [51]. In these decays, the final hadrons are produced in the form of pointlike color-singlet objects with a large relative momentum. Thus, the hadronization of the decay products occurs after they separate far away from each other. This provides the possibility to avoid the final state interaction. A more general treatment of factorization was presented in [58,59].

For the operators $\mathcal{O}_1 = (\bar{q}_1 q_2)_{V-A}(\bar{q}_1' q_2')_{V-A}$ and $\mathcal{O}_2 = (\bar{q}_1 q_2')_{V-A}(\bar{q}_1' q_2)_{V-A}$, using the Fierz transformation under which $V - A$ currents remain $V - A$ currents, one gets the following equivalent forms:

$$c_1\mathcal{O}_1 + c_2\mathcal{O}_2 = a_1\mathcal{O}_1 + c_2\tilde{\mathcal{O}}_2 = a_2\mathcal{O}_2 + c_1\tilde{\mathcal{O}}_1, \quad (5)$$

where

$$a_1(\mu) = c_1(\mu) + \frac{1}{N_c}c_2(\mu),$$
$$a_2(\mu) = c_2(\mu) + \frac{1}{N_c}c_1(\mu), \quad (6)$$

and N_c is the number of colors. The terms $\tilde{\mathcal{O}}_1 = (\bar{q}_1 T^a q_2')_{V-A}(\bar{q}_1' T^a q_2)_{V-A}$ and $\tilde{\mathcal{O}}_2 = (\bar{q}_1 T^a q_2)_{V-A} \times (\bar{q}_1' T^a q_2')_{V-A}$ with $SU(3)$ color generators T^a are the non-factorizable color-octet current operators, which are ne-

glected in the factorization assumption. A detailed analysis of $1/N_c$ corrections to the coefficients a_1, a_2 as well as the role of color-octet current operators in B decays can be found in [51].

In the factorization approach to nonleptonic meson decays, one can distinguish three classes of decays for which the amplitudes have the following general structure [50]:

$$\text{(class I): } \frac{G_F}{\sqrt{2}} V_{\text{CKM}} a_1(\mu) \langle \mathcal{O}_1 \rangle_F, \quad (7)$$

$$\text{(class II): } \frac{G_F}{\sqrt{2}} V_{\text{CKM}} a_2(\mu) \langle \mathcal{O}_2 \rangle_F, \quad (8)$$

$$\text{(class III): } \frac{G_F}{\sqrt{2}} V_{\text{CKM}} [a_1(\mu) + x a_2(\mu)] \langle \mathcal{O}_1 \rangle_F, \quad (9)$$

where $\langle \mathcal{O}_i \rangle_F$ represents the hadronic matrix element given as the products of matrix elements of quark currents and x is a nonperturbative factor equal to unity in the flavor symmetry limit [51]. The first (second) class is caused by a color-favored (color-suppressed) tree diagram and contains those decays in which only a charged (neutral) meson can be generated directly from a color-singlet current. The first and second class decay amplitudes are proportional to a_1 and a_2, respectively. The third class of transitions consists of those decays in which both a_1 and a_2 amplitudes interfere.

In this paper, we consider the following type of nonleptonic $B_c \rightarrow F_1 + F_2$, where F_1 is the pseudoscalar meson $(\eta_c, D_{(s)}, B_{(s)})$ and F_2 is the meson (vector or pseudoscalar) being factored out. For instance, the factorized matrix element of $B_c^+ \rightarrow F_1 F_2^+$ with $F_1 = \eta_c$ and $F_2 = \pi$ is defined as

$$X^{(B_c^+ F_1, F_2^+)} \equiv \langle F_1 | (\bar{c}b)_{V-A} | B_c \rangle \langle F_2 | (\bar{d}u)_{V-A} | 0 \rangle. \quad (10)$$

The matrix elements of the semileptonic $B_c \rightarrow F_1$ decays can be parametrized by two Lorentz-invariant form factors:

$$\langle F_1(P_2) | (\bar{q}q')_{V-A} | B_c(P_1) \rangle = f_+(q^2) P^\mu + f_-(q^2) q^\mu, \quad (11)$$

where $P = P_1 + P_2$ and $q = P_1 - P_2$. The two form factors also satisfy the following relation:

$$f_0(q^2) = f_+(q^2) + \frac{q^2}{M_1^2 - M_2^2} f_-(q^2). \quad (12)$$

The decay constants f_P and f_V of pseudoscalar (P) and vector (V) mesons are defined by

$$\langle P(p) | (\bar{q}q')_{V-A} | 0 \rangle = -i f_P p^\mu,$$
$$\langle V(p, h) | (\bar{q}q')_{V-A} | 0 \rangle = f_V M_V \epsilon^\mu(h), \quad (13)$$

where $\epsilon(h)$ is the polarization vector of the vector meson. In the above definitions for the decay constants, the ex-

perimental values of pion and rho meson decay constants are $f_\pi \approx 131$ MeV from $\pi \rightarrow \mu\nu$ and $f_\rho \approx 220$ MeV from $\rho \rightarrow e^+ e^-$.

Using Eqs. (11) and (13), we obtain the following expressions for the factorized matrix elements:

$$X^{(B_c^+ F_1, P^+)} = -i f_P (M_{B_c}^2 - M_{F_1}^2) f_0^{B_c \rightarrow F_1}(M_P^2), \quad (14)$$

when F_2 is a pseudoscalar meson, and

$$X^{(B_c^+ F_1, V^+)} = 2 f_V M_V (\epsilon \cdot P_{B_c}) f_+^{B_c \rightarrow F_1}(M_V^2), \quad (15)$$

when F_2 is a vector meson. For the latter case, only longitudinally polarized vector mesons are produced in the rest frame of the decaying B_c meson, i.e.,

$$\epsilon \cdot P_{B_c} = \frac{M_{B_c}}{M_V} p_c, \quad (16)$$

where

$$p_c = \frac{\sqrt{[M_{B_c}^2 - (M_1 + M_2)^2][M_{B_c}^2 - (M_1 - M_2)^2]}}{2M_{B_c}} \quad (17)$$

is the center of mass momentum of the final state meson (F_1 with M_1 or F_2 with M_2).

The decay rate for $B_c \rightarrow F_1 + F_2$ in the rest frame of the B_c meson is given by

$$\Gamma(B_c \rightarrow F_1 F_2) = \frac{p_c}{8\pi M_{B_c}^2} |\langle F_1 F_2 | \mathcal{H}_{\text{eff}} | B_c^+ \rangle|^2. \quad (18)$$

In Fig. 1, we show the example of quark diagrams for the nonleptonic $B_c \rightarrow BK$ decays: (a) color-favored (class I) $B_c^+ \rightarrow B^0 K^+$ and (b) color-suppressed (class II) $B_c^+ \rightarrow B^+ K^0$ decays. We also show in Fig. 2 the example of quark diagrams for the class III transitions such as $B_c \rightarrow D^+ D^0$.
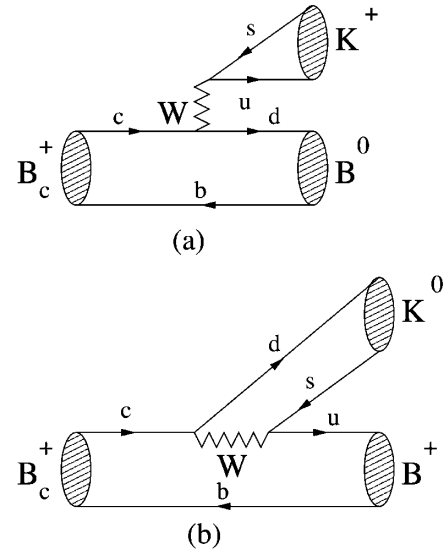

(a)

(b)

FIG. 1. Quark diagrams for the nonleptonic $B_c \rightarrow BK$ decays: (a) color-favored (class I) $B_c^+ \rightarrow B^0 K^+$ and (b) color-suppressed (class II) $B_c^+ \rightarrow B^+ K^0$ decays.
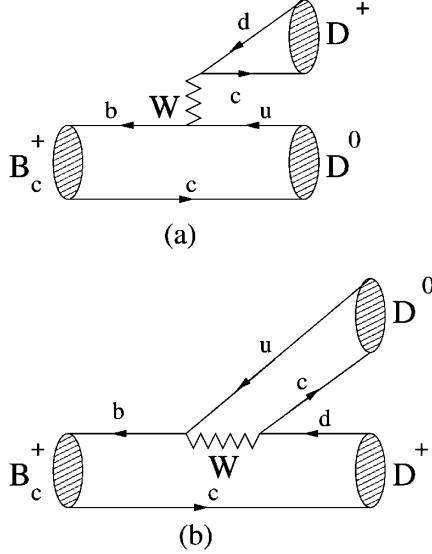
FIG. 2. Quark diagrams for the class III nonleptonic $B_c \to D^+ D^0$ decays, which consist of both color-favored (a) and color-suppressed (b) decays.

In the factorization approximation, these nonleptonic decay amplitudes can be expressed as the product of one-particle matrix elements.

A. Class I decay modes

(1) For the $b \to (u, c)(q_1 \bar{q}_2)$ process,

$$\langle D^0 M^+|\mathcal{H}_{\text{eff}}|B_c^+\rangle = \frac{G_F}{\sqrt{2}} V_{ub} V_{q_1 q_2}^* a_1 X^{(B_c^+ D^0, M^+)}$$

(19)

and

$$\langle \eta_c M^+|\mathcal{H}_{\text{eff}}|B_c^+\rangle = \frac{G_F}{\sqrt{2}} V_{cb} V_{q_1 q_2}^* a_1 X^{(B_c^+ \eta_c, M^+)}.$$

(20)

(2) For the $c \to (d, s)(q_1 \bar{q}_2)$ process,

$$\langle B^0 M^+|\mathcal{H}_{\text{eff}}|B_c^+\rangle = \frac{G_F}{\sqrt{2}} V_{cd} V_{q_1 q_2}^* a_1 X^{(B_c^+ B^0, M^+)}$$

(21)

and

$$\langle B_s^0 M^+|\mathcal{H}_{\text{eff}}|B_c^+\rangle = \frac{G_F}{\sqrt{2}} V_{cs} V_{q_1 q_2}^* a_1 X^{(B_c^+ B_s^0, M^+)},$$

(22)

where $M = \pi, K, \rho, K^*$ and $V_{q_1 q_2} = V_{ud}$ or V_{us} depending on whether $M = (\pi, \rho)$ or (K, K^*).

B. Class II decay modes

(1) For the $b \to (d, s)(q_1 \bar{q}_2)$ process,

$$\langle D^+ M^0|\mathcal{H}_{\text{eff}}|B_c^+\rangle = \frac{G_F}{\sqrt{2}} V_{q_2 b} V_{q_1 d}^* a_2 X^{(B_c^+ D^+, M^0)}$$

(23)

and

$$\langle D_s^+ M^0|\mathcal{H}_{\text{eff}}|B_c^+\rangle = \frac{G_F}{\sqrt{2}} V_{q_2 b} V_{q_1 s}^* a_2 X^{(B_c^+ D_s^+, M^0)}.$$

(24)

(2) For the $c \to u(q_1 \bar{q}_2)$ process,

$$\langle B^+ M^0|\mathcal{H}_{\text{eff}}|B_c^+\rangle = \frac{G_F}{\sqrt{2}} V_{cq_1} V_{uq_2}^* a_2 X^{(B_c^+ B^+, M^0)}$$

(25)

and

$$\langle B^+ \eta^{(\prime)}|\mathcal{H}_{\text{eff}}|B_c^+\rangle$$
$$= \frac{G_F}{\sqrt{2}} a_2 [V_{cd} V_{ud}^* X^{(B_c^+ B^+, \eta_q^{(\prime)})} + V_{cs} V_{us}^* X^{(B_c^+ B^+, \eta_s^{(\prime)})}],$$

(26)

where $M = (\pi, \eta^{(\prime)}, \rho, \omega, \bar{D}^{(*)})$ for $c \to (d, s)$ induced decays and $M = (\pi, \rho, \omega, K, \bar{K}, K^*, \bar{K}^*)$ for $c \to u$ induced decays, respectively. As in the case of color-favored class I decay modes, the factorized matrix elements for color-suppressed class II decay modes can be obtained from Eqs. (14) and (15) except that the decay constants for the neutral π^0, ρ^0, and ω mesons are replaced by $f_{P(V)}/\sqrt{2}$.

C. Class III decay modes

For the class III $B_c^+ \to D_q^+ M^0 (q = d, s)$ transitions, the decay amplitude is given by

$$\langle D_q^+ M^0|\mathcal{H}_{\text{eff}}|B_c^+\rangle$$
$$= \frac{G_F}{\sqrt{2}} V_{cq} V_F^* [a_1 X^{(B_c^+ M^0, D_q^+)} + a_2 X^{(B_c^+ D_q^+, M^0)}], \quad (27)$$

where $V_F = V_{cb}$ for $M = \eta_c$ and V_{ub} for $M = D$. The expressions for the factorized matrix elements can be obtained from Eqs. (14) and (15).

III. INPUT PARAMETERS

In this section we shall briefly discuss and summarize all of the input parameters, such as the model parameters, decay constants, and form factors for semileptonic $B_c \to (D_{(s)}, \eta_c, B_{(s)})$ decays, which are relevant to the present work.

A. Brief review of LFQM

The key idea in our LFQM [44,45] for the ground state mesons is to treat the radial wave function as a trial function for the variational principle to the QCD-motivated effective Hamiltonian saturating the Fock state expansion by the constituent quark and antiquark. The QCD-motivated effective Hamiltonian for a description of the ground state meson mass spectra is given by

$$H_{q\bar{q}} = H_0 + V_{q\bar{q}} = \sqrt{m_q^2 + \vec{k}^2} + \sqrt{m_{\bar{q}}^2 + \vec{k}^2} + V_{q\bar{q}}, \quad (28)$$

where

$$V_{q\bar{q}} = V_0 + V_{\text{hyp}} = a + br^n - \frac{4\alpha_s}{3r} + \frac{2}{3}\frac{\mathbf{S}_q \cdot \mathbf{S}_{\bar{q}}}{m_q m_{\bar{q}}}\nabla^2 V_{\text{Coul}}. \quad (29)$$

In this work, we use two interaction potentials: (1) the Coulomb plus linear confining (i.e. $n = 1$) potential and (2) the Coulomb plus harmonic oscillator (HO) (i.e. $n = 2$) potential, together with the hyperfine interaction $\langle\mathbf{S}_q \cdot \mathbf{S}_{\bar{q}}\rangle = 1/4(-3/4)$ for the vector (pseudoscalar) meson, which enables us to analyze the meson mass spectra and various wave-function-related observables, such as decay constants, electromagnetic form factors of mesons in a spacelike region, and the weak form factors for the exclusive semileptonic and rare decays of pseudoscalar mesons in the timelike region [44–49].

The momentum-space light-front wave function of the ground state pseudoscalar and vector mesons is given by $\Psi(x_i, \mathbf{k}_{i\perp}, \lambda_i) = \mathcal{R}_{\lambda_1\lambda_2}(x_i, \mathbf{k}_{i\perp})\phi(x_i, \mathbf{k}_{i\perp})$, where $\phi(x_i, \mathbf{k}_{i\perp})$ is the radial wave function and $\mathcal{R}_{\lambda_1\lambda_2}$ is the covariant spin-orbit wave function. The model wave function is represented by the Lorentz-invariant variables, $x_i = p_i^+/P^+$, $\mathbf{k}_{i\perp} = \mathbf{p}_{i\perp} - x_i\mathbf{P}_\perp$ and λ_i, where $P^\mu = (P^+, P^-, \mathbf{P}_\perp) = (P^0 + P^3, (M^2 + \mathbf{P}_\perp^2)/P^+, \mathbf{P}_\perp)$ is the momentum of the meson M, and p_i^μ and λ_i are the momenta and the helicities of constituent quarks, respectively.

The covariant forms of the spin-orbit wave functions for pseudoscalar and vector mesons are given by

$$\mathcal{R}_{\lambda_1\lambda_2}^{00} = \frac{-\bar{u}_{\lambda_1}(p_1)\gamma_5 v_{\lambda_2}(p_2)}{\sqrt{2}\tilde{M}_0},$$

$$\mathcal{R}_{\lambda_1\lambda_2}^{1J_z} = \frac{-\bar{u}_{\lambda_1}(p_1)[\not{\epsilon}(J_z) - \frac{\epsilon\cdot(p_1-p_2)}{M_0+m_1+m_2}]v_{\lambda_2}(p_2)}{\sqrt{2}\tilde{M}_0}, \quad (30)$$

where $\tilde{M}_0 = \sqrt{M_0^2 - (m_1 - m_2)^2}$, $M_0^2 = \sum_{i=1}^2(\mathbf{k}_{i\perp}^2 + m_i^2)/x_i$ is the boost invariant meson mass square obtained from the free energies of the constituents in mesons, and $\epsilon^\mu(J_z)$ is the polarization vector of the vector meson [60]. For the radial wave function ϕ, we use the same Gaussian wave function for both pseudoscalar and vector mesons:

$$\phi(x_i, \mathbf{k}_{i\perp}) = \frac{4\pi^{3/4}}{\beta^{3/2}}\sqrt{\frac{\partial k_z}{\partial x}}\exp(-\vec{k}^2/2\beta^2), \quad (31)$$

where β is the variational parameter and $\sqrt{\partial k_z/\partial x}$ is the Jacobian of the variable transformation $\{x, \mathbf{k}_\perp\} \rightarrow \vec{k} = (\mathbf{k}_\perp, k_z)$.

We apply our variational principle to the QCD-motivated effective Hamiltonian first to evaluate the expectation value of the central Hamiltonian $H_0 + V_0$, i.e., $\langle\phi|(H_0 + V_0)|\phi\rangle$, with a trial function $\phi(x_i, \mathbf{k}_{i\perp})$ that depends on the variational parameter β. Once the model parameters are fixed by minimizing the expectation value $\langle\phi|(H_0 + V_0)|\phi\rangle$, the mass eigenvalue of each meson is obtained as $M_{q\bar{q}} = \langle\phi|(H_0 + V_{q\bar{q}})|\phi\rangle$. Minimizing energies with respect to β and searching for a fit to the observed ground state meson spectra, our central potential V_0 obtained from our optimized potential parameters ($a = -0.72$ GeV, $b = 0.18$ GeV^2, and $\alpha_s = 0.31$) [44] for the Coulomb plus linear potential was found to be quite comparable with the quark potential model suggested by Scora and Isgur [61], where they obtained $a = -0.81$ GeV, $b = 0.18$ GeV^2, and $\alpha_s = 0.3 \sim 0.6$ for the Coulomb plus linear confining potential. A more detailed procedure for determining the model parameters of light- and heavy-quark sectors can be found in our previous works [44,45].

Our model parameters (m_q, $\beta_{q\bar{q}}$) obtained from the linear and HO potential models are summarized in Table II. The predictions of the ground state meson mass spectra, including bottom-charmed mesons, can be found in our recent work, Ref. [43].

B. Form factors for semileptonic $B_c \rightarrow P$ decays

For the nonleptonic two-body B_c decays, we use the q^2 dependent form factors $f_+(q^2)$ and $f_0(q^2)$ for the $B_c \rightarrow (D, D_s, \eta_c, B, B_s)$ decays as input parameters.

Within the framework of LF quantization, while the form factor $f_+(q^2)$ can be obtained only from the valence contribution in the $q^+ = 0$ frame with the "+" component of the currents without encountering the zero-mode con-

TABLE II. The constituent quark mass (GeV) and the Gaussian parameters β (GeV) for the linear and HO potentials obtained by the variational principle. $q = u$ and d.

Model	m_q	m_s	m_c	m_b	β_{qq}	β_{qs}	β_{ss}	β_{qc}	β_{sc}	β_{cc}	β_{qb}	β_{sb}	β_{cb}	β_{bb}
Linear	0.22	0.45	1.8	5.2	0.3659	0.3886	0.4128	0.4679	0.5016	0.6509	0.5266	0.5712	0.8068	1.1452
HO	0.25	0.48	1.8	5.2	0.3194	0.3419	0.3681	0.4216	0.4686	0.6998	0.4960	0.5740	1.0350	1.8025

tribution [62], the form factor $f_-(q^2)$ [or equivalently $f_0(q^2)$] receives the higher Fock state contribution (i.e., the zero mode in the $q^+ = 0$ frame or the nonvalence contribution in the $q^+ > 0$ frame). In order to calculate $f_-(q^2)$, we developed in [46,47] an effective treatment of handling the higher Fock state (or nonvalence) contribution to $f_-(q^2)$ in the purely longitudinal $q^+ > 0$ frame (i.e., $q^2 = q^+ q^- > 0$) based on the Bethe-Salpeter (BS) formalism. In our recent LFQM analysis [43] of the semileptonic $B_c \rightarrow (D, \eta_c, B, B_s)\ell\nu_\ell$ decays, we utilized our effective method [46] to express the zero-mode contribution as a convolution of a zero-mode operator with the initial and final state LF wave functions. In this way, we obtained the form factor $f_-(q^2)$ in the $q^+ = 0$ frame using the perpendicular components of the currents and discussed the LF covariance of $f_-(q^2)$ in the valence region by analyzing the covariant BS model and the LF covariant analysis described by Jaus [63].

The LF covariant form factors $f_+(q^2)$ and $f_-(q^2)$ for $B_c(q_1\bar{q}) \rightarrow P(q_2\bar{q})$ transitions obtained from the $q^+ = 0$ frame are given by (see [43] for more detailed derivations)

$$f_+(q^2) = \int_0^1 dx \int \frac{d^2\mathbf{k}_\perp}{16\pi^3} \frac{\phi_1(x, \mathbf{k}_\perp)}{\sqrt{\mathcal{A}_1^2 + \mathbf{k}_\perp^2}} \frac{\phi_2(x, \mathbf{k}_\perp')}{\sqrt{\mathcal{A}_2^2 + \mathbf{k}_\perp'^2}}$$
$$\times (\mathcal{A}_1 \mathcal{A}_2 + \mathbf{k}_\perp \cdot \mathbf{k}_\perp'),$$

$$f_-(q^2) = \int_0^1 (1-x)dx \int \frac{d^2\mathbf{k}_\perp}{16\pi^3} \frac{\phi_1(x, \mathbf{k}_\perp)}{\sqrt{\mathcal{A}_1^2 + \mathbf{k}_\perp^2}} \frac{\phi_2(x, \mathbf{k}_\perp')}{\sqrt{\mathcal{A}_2^2 + \mathbf{k}_\perp'^2}}$$
$$\times \left\{ -x(1-x)M_1^2 - \mathbf{k}_\perp^2 - m_1 m_{\bar{q}} \right.$$
$$+ (m_2 - m_{\bar{q}})\mathcal{A}_1 + 2\frac{q \cdot P}{q^2}\left[\mathbf{k}_\perp^2 + 2\frac{(\mathbf{k}_\perp \cdot \mathbf{q}_\perp)^2}{q^2} \right]$$
$$+ 2\frac{(\mathbf{k}_\perp \cdot \mathbf{q}_\perp)^2}{q^2} + \frac{\mathbf{k}_\perp \cdot \mathbf{q}_\perp}{q^2}$$
$$\times [M_2^2 - (1-x)(q^2 + q \cdot P) + 2xM_0^2$$
$$\left. - (1-2x)M_1^2 - 2(m_1 - m_{\bar{q}})(m_1 + m_2)] \right\}, \quad (32)$$

where $\mathbf{k}_\perp' = \mathbf{k}_\perp + (1-x)\mathbf{q}_\perp$, $\mathcal{A}_i = (1-x)m_i + xm_{\bar{q}}$ $(i = 1, 2)$, and $q \cdot P = M_1^2 - M_2^2$ with M_1 and M_2 being the physical masses of the initial and final state mesons, respectively. We should note that the LF covariant form factor $f_-(q^2)$ in Eq. (32) is the sum of the valence contribution $f_-^{\text{val}}(q^2)$ and the zero-mode contribution $f_-^{\text{Z.M.}}(q^2)$.

For the analysis of the nonleptonic $B_c \rightarrow D_s F$ decays where F is the vector or pseudoscalar meson being factored out, we show in Fig. 3 the q^2 dependence of the weak form factors $f_+(q^2)$ (solid line) and $f_0(q^2)$ (dashed line) for the $B_c \rightarrow D_s$ transition obtained from the linear (upper panel) and HO (lower panel) potential parameters. The circles represent the valence contribution $f_0^{\text{val}}(q^2)$ to $f_0(q^2)$. That is, the difference between $f_0(q^2)$ and $f_0^{\text{val}}(q^2)$ represents
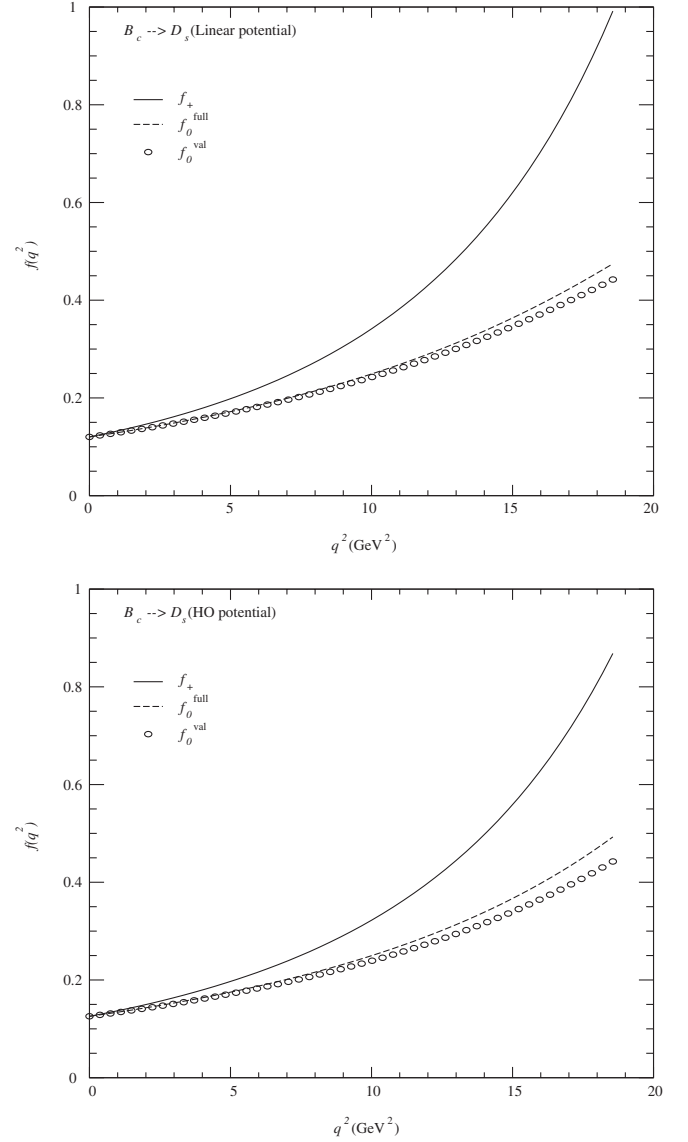
FIG. 3. The weak form factors $f_+(q^2)$ (solid line) and $f_0(q^2)$ (dashed line) for the $B_c \rightarrow D_s$ transition obtained from the linear (upper panel) and HO (lower panel) potential parameters. The circles represent the valence contributions $f_0^{\text{val}}(q^2)$ to $f_0(q^2)$.

the zero-mode contribution to $f_0(q^2)$. We obtain $f_+(0) = f_0(0) = 0.120$ [0.126] at $q^2 = 0$ for the linear [HO] potential model. The form factors at the zero-recoil point (i.e. $q^2 = q_{\text{max}}^2$) are obtained as $f_+(q_{\text{max}}^2) = 0.992$ [0.868] and $f_0(q_{\text{max}}^2) = 0.475$ [0.493] for the linear [HO] potential model. On the other hand, the valence contribution to $f_0(q^2)$ at the zero-recoil point is obtained as $f_0^{\text{val}}(q_{\text{max}}^2) = 0.442$ [0.443] for the linear [HO] potential model.

In Table III, we show the decay form factors $f_+(0) = f_0(0)$ at $q^2 = 0$ for the semileptonic $B_c \rightarrow (D, \eta_c, B, B_s)$ decays obtained from [43] and the rare $B_c \rightarrow D_s$ decay obtained in the present work (i.e. Fig. 3), and compare them to other theoretical model predictions.

TABLE III.   Form factors $f_+(0) = f_0(0)$ at $q^2 = 0$ for $B_c \rightarrow (D_{(s)}, \eta_c, B, B_s)$ transitions.

	Linear (HO)	[8,9]	[19]	[22]	[14]	[26]	[23]	[16]
$f_+^{B_c \rightarrow D}(0)$	0.086 [0.079]	0.14	0.69	0.1446	$\cdots$	0.089	0.16	0.08 ± 0.02
$f_+^{B_c \rightarrow D_s}(0)$	0.120 [0.126]	$\cdots$	$\cdots$	$\cdots$	$\cdots$	$\cdots$	0.28	0.15 ± 0.02
$F_+^{B_c \rightarrow \eta_c}(0)$	0.482 [0.546]	0.47	0.76	0.5359	0.49	0.622	0.61	0.58
$f_+^{B_c \rightarrow B}(0)$	0.467 [0.426]	0.39	0.58	0.4504	0.39	0.362	0.63	0.41 ± 0.04
$f_+^{B_c \rightarrow B_s}(0)$	0.573 [0.571]	0.50	0.61	0.5917	0.58	0.564	0.73	0.55 ± 0.03

C. Weak decay constants of η and η'

In this work, we shall also consider the nonleptonic decays of B_c mesons to isoscalar states such as ω and (η, η'). Isoscalar states with the same J^{PC} will mix, but mixing between the two light-quark isoscalar mesons and the much heavier charmonium or bottomonium states is generally assumed to be negligible. Since the vector mixing angle is known to be very close to ideal mixing, we assume ideal mixing between ω and ϕ mesons, i.e., $\omega = (u\bar{u} + d\bar{d})/\sqrt{2}$ and $\phi = s\bar{s}$. However, the octet-singlet mixing angle θ of η and η' is known to be in the range of $-10°$ to $-23°$. The physical η and η' are the mixtures of the flavor $SU(3)$ octet η_8 and singlet η_0 states:

$$\begin{pmatrix} \eta \\ \eta' \end{pmatrix} = U(\theta) \begin{pmatrix} \eta_8 \\ \eta_0 \end{pmatrix}, \qquad (33)$$

where

$$U(\theta) = \begin{pmatrix} \cos\theta & -\sin\theta \\ \sin\theta & \cos\theta \end{pmatrix}, \qquad (34)$$

and $\eta_8 = (u\bar{u} + d\bar{d} - 2s\bar{s})/\sqrt{6}$ and $\eta_0 = (u\bar{u} + d\bar{d} + s\bar{s})/\sqrt{3}$. Analogously, in terms of the quark-flavor basis $\eta_q = (u\bar{u} + d\bar{d})/\sqrt{2}$ and $\eta_s = s\bar{s}$, one obtains [64]

$$\begin{pmatrix} \eta \\ \eta' \end{pmatrix} = U(\phi) \begin{pmatrix} \eta_q \\ \eta_s \end{pmatrix}. \qquad (35)$$

The two schemes are equivalent to each other by $\phi = \theta + \arctan\sqrt{2}$ when $SU_f(3)$ symmetry is perfect. However, when one takes into account the $SU_f(3)$ breaking effect, this relationship is not maintained but given by the following Fock decompositions of the octet-singlet basis states [64]:

$$|\eta_8\rangle = \frac{\Psi_q + 2\Psi_s}{3} \frac{|u\bar{u} + d\bar{d} - 2s\bar{s}\rangle}{\sqrt{6}}$$
$$+ \frac{\sqrt{2}(\Psi_q - \Psi_s)}{3} \frac{|u\bar{u} + d\bar{d} + s\bar{s}\rangle}{\sqrt{3}},$$
$$|\eta_0\rangle = \frac{\sqrt{2}(\Psi_q - \Psi_s)}{3} \frac{|u\bar{u} + d\bar{d} - 2s\bar{s}\rangle}{\sqrt{6}} \qquad (36)$$
$$+ \frac{2\Psi_q + \Psi_s}{3} \frac{|u\bar{u} + d\bar{d} + s\bar{s}\rangle}{\sqrt{3}},$$

where Ψ_i denote LF wave functions of the corresponding parton states. Only in the $SU_f(3)$ symmetry limit, i.e., $\Psi_q = \Psi_s$, would one find pure octet and singlet states in Eq. (36). Although it was frequently assumed that the decay constants follow the same pattern of state mixing, the mixing properties of the decay constants will generally be different from the mixing properties of the meson state since the decay constants only probe the short-distance properties of the valence Fock states while the state mixing refers to the mixing of the overall wave function [64].

Using the decay constants of Eq. (13) defined in the quark-flavor basis, the two basic decay constants f_q and f_s arising from η_q and η_s are obtained as

$$f_{q(s)} = 2\sqrt{6} \int_0^1 dx \int \frac{d^2\mathbf{k}_\perp}{16\pi^3} \Psi_{q(s)}, \qquad (37)$$

and simply follow the pattern of state mixing due to the Okubo-Zweig-Iizuka rule [65], i.e.,

$$\begin{pmatrix} f_\eta^q & f_\eta^s \\ f_{\eta'}^q & f_{\eta'}^s \end{pmatrix} = U(\phi) \begin{pmatrix} f_q & 0 \\ 0 & f_s \end{pmatrix}. \qquad (38)$$

The Okubo-Zweig-Iizuka rule implies that the difference between the two mixing angles ϕ_q and ϕ_s vanishes [i.e., $\phi_q = \phi_s = \phi$ in Eq. (38)]. On the other hand, the decay constants in the octet-singlet basis are parametrized as [64,66]

$$\begin{pmatrix} f_\eta^8 & f_\eta^0 \\ f_{\eta'}^8 & f_{\eta'}^0 \end{pmatrix} = \begin{pmatrix} \cos\theta_8 & -\sin\theta_0 \\ \sin\theta_8 & \cos\theta_0 \end{pmatrix} \begin{pmatrix} f_8 & 0 \\ 0 & f_0 \end{pmatrix}, \qquad (39)$$

where θ_8 and θ_0 turn out to differ considerably and become equal only in the $SU_f(3)$ symmetry limit.

By using the correlation between the quark-flavor mixing scheme and the octet-singlet scheme [64,65], one obtains

$$f_8 = \sqrt{\frac{f_q^2 + 2f_s^2}{3}}, \qquad \theta_8 = \phi - \arctan(\sqrt{2}f_s/f_q),$$
$$f_0 = \sqrt{\frac{2f_q^2 + f_s^2}{3}}, \qquad \theta_0 = \phi - \arctan(\sqrt{2}f_q/f_s). \qquad (40)$$

In our previous work [44], we obtained the $\eta - \eta'$ mixing angle $\theta \simeq -19°$ for both linear and HO potential models by fitting the physical masses of η and η'. This corresponds to the mixing angle $\phi = 35.7°$ in the quark-flavor

TABLE IV.   Meson decay constants (in units of MeV) used in this work.

f_π	f_K	f_ρ	f_ω	f_{K^*}	f_η^q	f_η^s	$f_{\eta'}^q$	$f_{\eta'}^s$	f_D	f_{D^*}	f_{η_c}	f_{D_s}
131 [57]	159.8 [57]	220 [57]	195 [57]	217 [57]	104.8	−110.3	75.3	150.0	222.6 [68]	241 [48]	340 [48]	259.5 [69]

basis. We applied this mixing angle to predict the decay widths for $\eta(\eta') \to \gamma\gamma$ using the axial anomaly plus partial conservation of the axial vector current (PCAC) relations [67] and obtained $f_8/f_\pi = 1.32(1.25)$ and $f_0/f_\pi = 1.16(1.13)$ for the linear (HO) potential model [44]. From the decay constants of octet and singlet mesons together with Eq. (40), we now obtain the four parameters $(f_q, f_s, \theta_8, \theta_0)$ as follows: $f_q/f_\pi = 0.97\,(1.00)$, $f_s/f_\pi = 1.46(1.36)$, $\theta_8 = -29.2°\,(-26.8°)$, and $\theta_0 = -7.3°\,(-10.6°)$ for the linear (HO) potential model, respectively. Given this background, we finally obtain the decay constants related to the η and η' mesons as follows:

$$f_\eta^q = 103.2\,(106.4)\ \text{MeV},$$
$$f_\eta^s = -116.6\,(-104.0)\ \text{MeV},$$
$$f_{\eta'}^q = 74.2\,(76.4)\ \text{MeV}, \tag{41}$$
$$f_{\eta'}^s = 155.3\,(144.7)\ \text{MeV}.$$

Our results for the mixing parameters of η and η' are consistent with those obtained from Feldmann et al. [64], namely, $f_8/f_\pi = 1.26$, $f_0/f_\pi = 1.17$, $f_q/f_\pi = (1.07 \pm 0.02)$, $f_s/f_\pi = (1.34 \pm 0.06)$, $\phi = (39.3° \pm 1.0°)$, $\theta_8 = -21.2°$, $\theta_0 = -9.2°$, $f_\eta^q = (108.5 \pm 2.0)$ MeV, $f_\eta^s = -(111.2 \pm 5.0)$ MeV, $f_{\eta'}^q = (88.8 \pm 1.7)$ MeV, and $f_{\eta'}^s = (135.8 \pm 6.1)$ MeV.

For the measured values of meson decay constants, we use the central values extracted from the experimental measurements [57,68,69]. However, for the unmeasured decay constants, we use the average values obtained from our linear and HO model predictions in [48] in addition to the present work. The values for the decay constants used in this work are compiled in Table IV. Since the decay constant f_{η_c} extracted from CLEO Collaboration [70] has a large error bar, i.e., $f_{\eta_c}^{\text{CLEO}} = 335 \pm 75$ MeV, we instead take the average value $f_{\eta_c} = 340$ MeV of our LFQM predictions [48], i.e., $f_{\eta_c}^{\text{lin}} = 326$ MeV and $f_{\eta_c}^{\text{HO}} = 354$ MeV.

IV. NUMERICAL RESULTS

In our numerical calculations of exclusive B_c decays, we use two sets of model parameters (m, β) for the linear and HO confining potentials given in Table II to compute the weak form factors for semileptonic $B_c \to (D_{(s)}, \eta_c, B_{(s)})$ decays and the unmeasured decay constants as given in Tables III and IV, respectively. Using them together with the CKM matrix elements given by Table I, we finally predict the branching ratios which are given in Tables V

and VI. Although we show the form factors in Table III only at a maximum recoil point $q^2 = 0$, we use the form factor at $q^2 = M_F^2$ obtained from [43] for the corresponding nonleptonic $B_c \to (D_{(s)}, \eta_c, B_{(s)})M_F$ decays.

In Table V we show the nonleptonic decay widths of the B_c meson for a general value of the Wilson coefficients a_1 and a_2, whereas in Table VI we give the corresponding branching ratios (in %) at the fixed choice of Wilson coefficients [5], $a_1^c(a_1^b) = 1.20\,(1.14)$ and $a_2^c(a_2^b) = -0.317\,(-0.20)$, relevant for the nonleptonic decays of the $c(\bar{b})$ quark. For the lifetime of the B_c, we take the central value $\tau(B_c) = 0.46$ ps (i.e. $\Gamma_{\text{tot}} = 1.43 \times 10^{-12}$ GeV) presented by PDG [57]. Our branching ratios for both b and c induced decays listed in Table VI are generally close to the other quark model results [7–9,14,26] but differ substantially from the ones obtained by Refs. [5,10,40].

The relative size of the branching ratios for various decay modes may be estimated from power counting of the Wilson coefficients a_i and the CKM factors with respect to the small parameter of the Cabibbo angle $\lambda = \sin\theta_C$ in the Wolfenstein parametrization [71]; e.g. the CKM matrix elements can be expanded in terms of λ as $V_{ud} \sim 1$, $V_{us} \sim \lambda$, $V_{ub} \sim \lambda^3$, $V_{cd} \sim -\lambda$, $V_{cs} \sim 1$, and $V_{cb} \sim \lambda^2$. From Tables V and VI, we make the following observations:

(1) The class I decay modes determined by the Wilson coefficient a_1 have comparatively large branching ratios. The CKM favored c decays such as $B_c^+ \to B_s^0(\pi^+, \rho^+)$ decays with the CKM factor $V_{cs}V_{ud}^* \sim \lambda^0$ have branching ratios of the order of 10^{-2} (e.g. 2%–4% in our model predictions), which are the most promising class I decay modes shown in Tables V and VI. The CKM-suppressed c decays such as $B_c^+ \to B_s^0 K^+$ with $V_{cs}V_{us}^* \sim \lambda^1$ and $B_c^+ \to B^0(\pi^+, \rho^+)$ with $V_{cd}V_{ud}^* \sim \lambda^1$, as well as the CKM-suppressed b decays such as $B_c^+ \to \eta_c(\pi^+, \rho^+)$ with $V_{cb}V_{ud}^* \sim \lambda^2$, have branching ratios of the order of 10^{-3} and should still be accessible at high luminosity hadron colliders. However, the branching ratios of the $b \to u$ induced decay modes are too small $\mathcal{O}(10^{-8}$–$10^{-6})$ to be measured experimentally.

(2) The branching ratios for the class II decay modes determined by a_2 are relatively smaller than those for the class I decay modes. However, the $B_c^+ \to B^+(\bar{K}^0, \bar{K}^{*0})$ decays with $V_{cs}V_{ud}^* \sim \lambda^0$ have branching ratios of the order of 10^{-3} and these modes should be accessible experimentally. Of interest is

TABLE V.　Exclusive nonleptonic decay widths Γ (in 10^{-15} GeV) of the B_c meson for the general values of the Wilson coefficients a_1 and a_2.

Class	Mode	Linear (HO)	[8,9]	[14]	[26]
I	$B_c^+ \to D^0\pi^+$	$4.7[4.7](\times10^{-4})a_1^2$	$\cdots$	$\cdots$	$\cdots$
	$B_c^+ \to D^0\rho^+$	$1.4[1.2](\times10^{-3})a_1^2$	$\cdots$	$\cdots$	$\cdots$
	$B_c^+ \to D^0K^+$	$3.9[3.4](\times10^{-5})a_1^2$	$\cdots$	$\cdots$	$\cdots$
	$B_c^+ \to D^0K^{*+}$	$7.5[6.4](\times10^{-5})a_1^2$	$\cdots$	$\cdots$	$\cdots$
	$B_c^+ \to \eta_c\pi^+$	$0.997[1.280]a_1^2$	$0.93a_1^2$	$1.02a_1^2$	$1.47a_1^2$
	$B_c^+ \to \eta_c\rho^+$	$2.827[3.563]a_1^2$	$2.3a_1^2$	$2.60a_1^2$	$3.35a_1^2$
	$B_c^+ \to \eta_cK^+$	$0.081[0.103]a_1^2$	$0.073a_1^2$	$0.082a_1^2$	$0.15a_1^2$
	$B_c^+ \to \eta_cK^{*+}$	$0.147[0.184]a_1^2$	$0.12a_1^2$	$0.15a_1^2$	$0.24a_1^2$
	$B_c^+ \to B^0\pi^+$	$1.557[1.296]a_1^2$	$1.0a_1^2$	$1.10a_1^2$	$1.51a_1^2$
	$B_c^+ \to B^0\rho^+$	$1.936[1.505]a_1^2$	$1.3a_1^2$	$1.41a_1^2$	$1.93a_1^2$
	$B_c^+ \to B^0K^+$	$0.126[0.104]a_1^2$	$0.09a_1^2$	$0.098a_1^2$	$\cdots$
	$B_c^+ \to B^0K^{*+}$	$0.042[0.032]a_1^2$	$0.04a_1^2$	$0.038a_1^2$	$\cdots$
	$B_c^+ \to B_s^0\pi^+$	$36.97[36.71]a_1^2$	$25a_1^2$	$34.7a_1^2$	$34.78a_1^2$
	$B_c^+ \to B_s^0\rho^+$	$25.43[23.22]a_1^2$	$14a_1^2$	$23.1a_1^2$	$23.61a_1^2$
	$B_c^+ \to B_s^0K^+$	$2.853[2.816]a_1^2$	$2.1a_1^2$	$2.87a_1^2$	$\cdots$
	$B_c^+ \to B_s^0K^{*+}$	$0.069[0.061]a_1^2$	$0.03a_1^2$	$0.13a_1^2$	$\cdots$
II	$B_c^+ \to D^+\pi^0$	$2.4[2.0](\times10^{-4})a_2^2$	$\cdots$	$\cdots$	$\cdots$
	$B_c^+ \to D^+\rho^0$	$7.0[6.0](\times10^{-4})a_2^2$	$\cdots$	$\cdots$	$\cdots$
	$B_c^+ \to D^+\omega$	$5.5[4.7](\times10^{-4})a_2^2$	$\cdots$	$\cdots$	$\cdots$
	$B_c^+ \to D^+\eta$	$3.1[2.7](\times10^{-4})a_2^2$	$\cdots$	$\cdots$	$\cdots$
	$B_c^+ \to D^+\eta'$	$1.7[1.5](\times10^{-5})a_2^2$	$\cdots$	$\cdots$	$\cdots$
	$B_c^+ \to D^+\bar{D}^0$	$0.219[0.185]a_2^2$	$\cdots$	$\cdots$	$\cdots$
	$B_c^+ \to D^+\bar{D}^{*0}$	$0.261[0.212]a_2^2$	$\cdots$	$\cdots$	$\cdots$
	$B_c^+ \to D_s^+\pi^0$	$2.4[2.6](\times10^{-5})a_2^2$	$\cdots$	$\cdots$	$\cdots$
	$B_c^+ \to D_s^+\rho^0$	$7.1[7.6](\times10^{-5})a_2^2$	$\cdots$	$\cdots$	$\cdots$
	$B_c^+ \to D_s^+\omega$	$5.6[6.0](\times10^{-5})a_2^2$	$\cdots$	$\cdots$	$\cdots$
	$B_c^+ \to D_s^+\eta$	$3.2[3.4](\times10^{-5})a_2^2$	$\cdots$	$\cdots$	$\cdots$
	$B_c^+ \to D_s^+\eta'$	$1.7[1.9](\times10^{-5})a_2^2$	$\cdots$	$\cdots$	$\cdots$
	$B_c^+ \to D_s^+\bar{D}^0$	$0.0216[0.0227]a_2^2$	$\cdots$	$\cdots$	$\cdots$
	$B_c^+ \to D_s^+\bar{D}^{*0}$	$0.0248[0.0250]a_2^2$	$\cdots$	$\cdots$	$\cdots$
	$B_c^+ \to B^+\pi^0$	$0.779[0.648]a_2^2$	$0.5a_2^2$	$0.54a_2^2$	$1.03a_2^2$
	$B_c^+ \to B^+\rho^0$	$0.967[0.752]a_2^2$	$0.7a_2^2$	$0.71a_2^2$	$1.28a_2^2$
	$B_c^+ \to B^+\omega$	$0.721[0.558]a_2^2$	$\cdots$	$\cdots$	$\cdots$
	$B_c^+ \to B^+\eta$	$3.99[3.30]a_2^2$	$\cdots$	$\cdots$	$\cdots$
	$B_c^+ \to B^+\eta'$	$0.054[0.045]a_2^2$	$\cdots$	$\cdots$	$\cdots$
	$B_c^+ \to B^+K^0$	$0.125[0.104]a_2^2$	$\cdots$	$\cdots$	$\cdots$
	$B_c^+ \to B^+\bar{K}^0$	$47.85[39.66]a_2^2$	$34a_2^2$	$35.3a_2^2$	$\cdots$
	$B_c^+ \to B^+K^{*0}$	$0.040[0.030]a_2^2$	$\cdots$	$\cdots$	$\cdots$
	$B_c^+ \to B^+\bar{K}^{*0}$	$15.36[11.38]a_2^2$	$13a_2^2$	$13.1a_2^2$	$\cdots$
III	$B_c^+ \to D^+D^0$	$(0.011a_1 + 0.011a_2)^2[(0.0097a_1 + 0.0097a_2)^2]$	$\cdots$	$\cdots$	$\cdots$
	$B_c^+ \to D_s^+D^0$	$(0.058a_1 + 0.064a_2)^2[(0.052a_1 + 0.066a_2)^2]$	$\cdots$	$\cdots$	$\cdots$
	$B_c^+ \to \eta_cD^+$	$(0.428a_1 + 0.226a_2)^2[(0.482a_1 + 0.208a_2)^2]$	$\cdots$	$(0.438a_1 + 0.236a_2)^2$	$(0.47a_1 + 0.73a_2)^2$
	$B_c^+ \to \eta_cD_s^+$	$(2.27a_1 + 1.32a_2)^2[(2.47a_1 + 1.34a_2)^2]$	$\cdots$	$(2.54a_1 + 1.93a_2)^2$	$(2.59a_1 + 3.40a_2)^2$

the abnormally small branching ratio of $B_c^+ \to B^+\eta'$ compared to that of $B_c^+ \to B^+\eta$. As stated in [40], the reason for such a small branching ratio is not only because the available physical phase space is too small but also because there are large destructive interferences between η'_q and η'_s due to the serious cancellation between the CKM factors $V_{cd}V_{ud}^*$ and $V_{cs}V_{us}^*$.

(3) The class III decay modes involve the Pauli interference. Taking into account the negative value of a_2 with respect to a_1, one can see that the class III decay modes shown in Table V should be suppressed in comparison with the cases in which the interference is switched off. In order to test the effects of the interference, one may put the widths in the form of $\Gamma = \Gamma_0 + \Delta\Gamma$, where $\Gamma_0 = x_1a_1^2 + x_2a_2^2$

TABLE VI. Branching ratios (in %) of the exclusive nonleptonic B_c decays at the fixed choice of Wilson coefficients, $a_1^c(a_1^b) = 1.20(1.14)$ and $a_2^c(a_2^b) = -0.317(-0.20)$, relevant for the nonleptonic decays of the $c(\bar{b})$ quark. For the lifetime of the B_c we take $\tau(B_c) = 0.46$ ps.

Class	Mode	Linear (HO)	[8,9]	[14]	[26]	[7]	[5]	[13]	[40]	[10]
I	$B_c^+ \to D^0\pi^+$	$4.3[4.3](\times10^{-5})$	$\cdots$	$\cdots$	$\cdots$	$\cdots$	$\cdots$	$\cdots$	$\cdots$	$\cdots$
	$B_c^+ \to D^0\rho^+$	$1.3[1.1](\times10^{-4})$	$\cdots$	$\cdots$	$\cdots$	$\cdots$	$\cdots$	$\cdots$	$\cdots$	$\cdots$
	$B_c^+ \to D^0K^+$	$3.5[3.1](\times10^{-6})$	$\cdots$	$\cdots$	$\cdots$	$\cdots$	$\cdots$	$\cdots$	$\cdots$	$\cdots$
	$B_c^+ \to D^0K^{*+}$	$6.8[5.8](\times10^{-6})$	$\cdots$	$\cdots$	$\cdots$	$\cdots$	$\cdots$	$\cdots$	$\cdots$	$\cdots$
	$B_c^+ \to \eta_c\pi^+$	$0.091[0.116]$	0.085	0.094	0.13	0.19	0.20	0.025	$\cdots$	0.18
	$B_c^+ \to \eta_c\rho^+$	$0.257[0.324]$	0.21	0.24	0.30	0.45	0.42	0.067	$\cdots$	0.49
	$B_c^+ \to \eta_cK^+$	$0.0074[0.0094]$	0.0075	0.0075	0.013	0.015	0.013	0.002	$\cdots$	0.014
	$B_c^+ \to \eta_cK^{*+}$	$0.013[0.017]$	0.011	0.013	0.021	0.025	0.020	0.004	$\cdots$	0.025
	$B_c^+ \to B^0\pi^+$	$0.157[0.131]$	0.10	0.11	0.15	0.20	1.06	0.19	0.373	0.32
	$B_c^+ \to B^0\rho^+$	$0.195[0.152]$	0.13	0.14	0.19	0.20	0.96	0.15	0.527	0.59
	$B_c^+ \to B^0K^+$	$0.013[0.011]$	0.009	0.010	$\cdots$	0.015	0.07	0.014	0.027	0.025
	$B_c^+ \to B^0K^{*+}$	$0.0042[0.0032]$	0.004	0.0039	$\cdots$	0.0048	0.015	0.003	0.023	0.018
	$B_c^+ \to B_s^0\pi^+$	$3.723[3.697]$	2.52	3.51	3.42	3.9	16.4	3.01	5.309	5.75
	$B_c^+ \to B_s^0\rho^+$	$2.561[2.338]$	1.41	2.34	2.33	2.3	7.2	1.34	6.265	4.41
	$B_c^+ \to B_s^0K^+$	$0.287[0.284]$	0.21	0.29	$\cdots$	0.29	1.06	0.21	0.367	0.41
	$B_c^+ \to B_s^0K^{*+}$	$0.0069[0.0061]$	0.003	0.013	$\cdots$	0.011	$\cdots$	0.0043	0.165	$\cdots$
II	$B_c^+ \to D^+\pi^0$	$6.7[5.6](\times10^{-7})$	$\cdots$	$\cdots$	$\cdots$	$\cdots$	$\cdots$	$\cdots$	$\cdots$	$\cdots$
	$B_c^+ \to D^+\rho^0$	$2.0[1.7](\times10^{-6})$	$\cdots$	$\cdots$	$\cdots$	$\cdots$	$\cdots$	$\cdots$	$\cdots$	$\cdots$
	$B_c^+ \to D^+\omega$	$1.5[1.3](\times10^{-6})$	$\cdots$	$\cdots$	$\cdots$	$\cdots$	$\cdots$	$\cdots$	$\cdots$	$\cdots$
	$B_c^+ \to D^+\eta$	$8.7[7.6](\times10^{-7})$	$\cdots$	$\cdots$	$\cdots$	$\cdots$	$\cdots$	$\cdots$	$\cdots$	$\cdots$
	$B_c^+ \to D^+\eta'$	$4.8[4.2](\times10^{-8})$	$\cdots$	$\cdots$	$\cdots$	$\cdots$	$\cdots$	$\cdots$	$\cdots$	$\cdots$
	$B_c^+ \to D^+\bar{D}^0$	$6.1[5.2](\times10^{-4})$	$\cdots$	$\cdots$	$\cdots$	3.3×10^{-3}	5.3×10^{-3}	4.1×10^{-4}	$\cdots$	1.8×10^{-3}
	$B_c^+ \to D^+\bar{D}^{*0}$	$7.3[5.9](\times10^{-4})$	$\cdots$	$\cdots$	$\cdots$	3.8×10^{-3}	7.5×10^{-3}	3.6×10^{-4}	$\cdots$	1.9×10^{-3}
	$B_c^+ \to D_s^+\pi^0$	$6.7[7.3](\times10^{-8})$	$\cdots$	$\cdots$	$\cdots$	$\cdots$	$\cdots$	$\cdots$	$\cdots$	$\cdots$
	$B_c^+ \to D_s^+\rho^0$	$2.0[2.1](\times10^{-7})$	$\cdots$	$\cdots$	$\cdots$	$\cdots$	$\cdots$	$\cdots$	$\cdots$	$\cdots$
	$B_c^+ \to D_s^+\omega$	$1.6[1.7](\times10^{-7})$	$\cdots$	$\cdots$	$\cdots$	$\cdots$	$\cdots$	$\cdots$	$\cdots$	$\cdots$
	$B_c^+ \to D_s^+\eta$	$9.0[9.5](\times10^{-8})$	$\cdots$	$\cdots$	$\cdots$	$\cdots$	$\cdots$	$\cdots$	$\cdots$	$\cdots$
	$B_c^+ \to D_s^+\eta'$	$4.8[5.3](\times10^{-8})$	$\cdots$	$\cdots$	$\cdots$	$\cdots$	$\cdots$	$\cdots$	$\cdots$	$\cdots$
	$B_c^+ \to D_s^+\bar{D}^0$	$6.0[6.3](\times10^{-5})$	$\cdots$	$\cdots$	$\cdots$	2.1×10^{-4}	4.8×10^{-4}	2.7×10^{-5}	$\cdots$	9.3×10^{-5}
	$B_c^+ \to D_s^+\bar{D}^{*0}$	$6.9[7.0](\times10^{-5})$	$\cdots$	$\cdots$	$\cdots$	2.4×10^{-4}	7.1×10^{-4}	2.5×10^{-5}	$\cdots$	9.7×10^{-5}
	$B_c^+ \to B^+\pi^0$	$0.0055[0.0046]$	0.004	0.0038	0.007	0.007	0.037	$\cdots$	4.6×10^{-5}	0.011
	$B_c^+ \to B^+\rho^0$	$0.0068[0.0053]$	0.005	0.0050	0.009	0.0071	0.034	$\cdots$	6.5×10^{-5}	0.020
	$B_c^+ \to B^+\omega$	$0.0051[0.0039]$	$\cdots$	$\cdots$	$\cdots$	$\cdots$	$\cdots$	$\cdots$	5.8×10^{-5}	$\cdots$
	$B_c^+ \to B^+\eta$	$0.028[0.023]$	$\cdots$	$\cdots$	$\cdots$	$\cdots$	$\cdots$	$\cdots$	1.6×10^{-4}	$\cdots$
	$B_c^+ \to B^+\eta'$	$3.8[3.2](\times10^{-4})$	$\cdots$	$\cdots$	$\cdots$	$\cdots$	$\cdots$	$\cdots$	8.9×10^{-6}	$\cdots$
	$B_c^+ \to B^+K^0$	$8.8[7.3](\times10^{-4})$	$\cdots$	$\cdots$	$\cdots$	$\cdots$	$\cdots$	$\cdots$	6.5×10^{-6}	$\cdots$
	$B_c^+ \to B^+\bar{K}^0$	$0.336[0.279]$	0.24	0.25	$\cdots$	0.38	1.98	$\cdots$	0.0022	0.66
	$B_c^+ \to B^+K^{*0}$	$2.8[2.1](\times10^{-4})$	$\cdots$	$\cdots$	$\cdots$	$\cdots$	$\cdots$	$\cdots$	5.5×10^{-6}	$\cdots$
	$B_c^+ \to B^+\bar{K}^{*0}$	$0.108[0.080]$	0.09	0.093	$\cdots$	0.11	0.43	$\cdots$	0.0018	0.47
III	$B_c^+ \to D^+D^0$	$7.5[5.8](\times10^{-6})$	$\cdots$	$\cdots$	$\cdots$	3.1×10^{-5}	3.2×10^{-5}	$\cdots$	$\cdots$	$\cdots$
	$B_c^+ \to D_s^+D^0$	$2.0[1.5](\times10^{-4})$	$\cdots$	$\cdots$	$\cdots$	7.4×10^{-4}	6.6×10^{-4}	$\cdots$	$\cdots$	$\cdots$
	$B_c^+ \to \eta_cD^+$	$0.014[0.018]$	$\cdots$	0.014	0.010	0.019	0.032	0.0055	$\cdots$	0.0012
	$B_c^+ \to \eta_cD_s^+$	$0.378[0.454]$	$\cdots$	0.44	0.35	0.44	0.86	0.51	$\cdots$	0.056

and $\Delta\Gamma = za_1a_2$, and then compute the $\Delta\Gamma/\Gamma_0$ (in %) as done in [5]. Our absolute values of $\Delta\Gamma/\Gamma_0$ obtained from the linear (HO) model are 34.0 (34.0)% for $B_c^+ \to D^+D^0$, 37.3 (42.4)% for $B_c^+ \to D_s^+D^0$, 18.4 (15.1)% for $B_c^+ \to \eta_cD^+$, and 20.2 (18.9)% for $B_c^+ \to \eta_cD_s^+$, respectively. This

indicates that the interference is the most significantly involved in the $B_c^+ \to D_s^+D^0$ decay compared to others. In particular, the $B_s^+ \to D_s^+D^0$ and $B_c^+ \to D_s^+\bar{D}_0$ decay modes have been proposed in [29,33,38,41] for the extraction of the CKM angle γ through amplitude relations.

V. SUMMARY

In this work, we have studied the exclusive nonleptonic $B_c \to (D_{(s)}, \eta_c, B_{(s)})M$ decays, where the final state M mesons are factored out in the QCD factorization approach. The inputs used to obtain their branching ratios were the weak form factors for the semileptonic $B_c \to (D_{(s)}, \eta_c, B_{(s)})$ decays in the whole kinematical region and the unmeasured weak decay constants obtained from our previous LFQM analysis [43–45,48]. For the measured values of decay constants, we use the central values extracted from the experimental measurements [57,68,69].

Our predictions for the branching ratios are summarized in Tables V and VI and compared with other theoretical results. Overall, the class II decay modes have more discrepancies among the theoretical models than the class I and III decay modes do. The upcoming experimental mea-surements of the corresponding decay rates can examine various theoretical approaches. The most promising measurable decay modes appear to be the CKM favored c decays such as $B_c^+ \to B_s^0(\pi^+, \rho^+)$ decays. It is thus expected that the dominant contribution to the B_c total rate comes from the c induced decays. The more c induced $B_c \to VP$ and $B_c \to VV$ decay modes seem to deserve further consideration.

[1] F. Abe *et al.* (CDF Collaboration), Phys. Rev. D **58,** 112004 (1998); Phys. Rev. Lett. **81,** 2432 (1998).

[2] A. Abulencia *et al.* (CDF Collaboration), Phys. Rev. Lett. **97,** 012002 (2006); T. Aaltonen *et al.* (CDF Collaboration), Phys. Rev. Lett. **100,** 182002 (2008).

[3] V. M. Abazov *et al.* (D0 Collaboration), Phys. Rev. Lett. **101,** 012001 (2008).

[4] N. Brambilla *et al.* (Quarkoninum Working Group), Report No. CERN-2005-005; M. P. Altarelli and F. Teubert, Int. J. Mod. Phys. A **23,** 5117 (2008).

[5] I. P. Gouz, V. V. Kiselev, A. K. Likhoded, V. I. Romanovsky, and O. P. Yushchenko, Yad. Fiz. **67,** 1581 (2004) [Phys. At. Nucl. **67,** 1559 (2004)].

[6] V. V. Kiselev, A. E. Kovalsky, and A. K. Likhoded, Nucl. Phys. **B585,** 353 (2000); V. V. Kiselev, A. K. Likhoded, and A. I. Onishchenko, Nucl. Phys. **B569,** 473 (2000).

[7] M. A. Ivanov, J. G. Körner, and P. Santorelli, Phys. Rev. D **73,** 054024 (2006).

[8] D. Ebert, R. N. Faustov, and V. O. Galkin, Phys. Rev. D **68,** 094020 (2003).

[9] D. Ebert, R. N. Faustov, and V. O. Galkin, Eur. Phys. J. C **32,** 29 (2003).

[10] C.-H. Chang and Y.-Q. Chen, Phys. Rev. D **49,** 3399 (1994).

[11] J.-F. Liu and K.-T. Chao, Phys. Rev. D **56,** 4133 (1997).

[12] A. Abd El-Hady, J. H. Munoz, and J. P. Vary, Phys. Rev. D **62,** 014019 (2000).

[13] P. Colangelo and F. De Fazio, Phys. Rev. D **61,** 034012 (2000).

[14] E. Hernández, J. Nieves, and J. M. Verde-Velasco, Phys. Rev. D **74,** 074008 (2006).

[15] D. Du and Z. Wang, Phys. Rev. D **39,** 1342 (1989).

[16] R. Dhir, N. Sharma, and R. C. Verma, J. Phys. G **35,** 085002 (2008).

[17] P. Colangelo, G. Nardulli, and N. Paver, Z. Phys. C **57,** 43 (1993).

[18] T. Huang and F. Zuo, Eur. Phys. J. C **51,** 833 (2007).

[19] M. A. Ivanov, J. G. Körner, and P. Santorelli, Phys. Rev. D **63,** 074010 (2001).

[20] M. A. Ivanov, J. G. Körner, and P. Santorelli, Phys. Rev. D **71,** 094006 (2005).

[21] D. Ebert, R. N. Faustov, and V. O. Galkin, Phys. Rev. D **67,** 014027 (2003).

[22] M. A. Nobes and R. M. Woloshyn, J. Phys. G **26,** 1079 (2000).

[23] W. Wang, Y.-L. Shen, and C.-D. Lü, Phys. Rev. D **79,** 054012 (2009).

[24] M. Lusignoli and M. Masetti, Z. Phys. C **51,** 549 (1991).

[25] S. Godfrey, Phys. Rev. D **70,** 054017 (2004).

[26] A. Yu. Anisimov, P. Yu. Kulikov, I. M. Narodetskii, and K. A. Ter-Martirosyan, Yad. Fiz. **62,** 1868 (1999) [Phys. At. Nucl. **62,** 1739 (1999)].

[27] R. C. Verma and A. Sharma, Phys. Rev. D **65,** 114007 (2002); **64,** 114018 (2001).

[28] A. K. Giri, B. Mawlong, and R. Mohanta, Phys. Rev. D **75,** 097304 (2007); **76,** 099902(E) (2007); A. K. Giri, R. Mohanta, and M. P. Khanna, Phys. Rev. D **65,** 034016 (2002).

[29] V. V. Kiselev, J. Phys. G **30,** 1445 (2004).

[30] X. Liu and X. Q. Li, Phys. Rev. D **77,** 096010 (2008).

[31] J. F. Cheng, D. S. Du, and C. D. Lü, Eur. Phys. J. C **45,** 711 (2006).

[32] S. Fajfer, J. F. Kamenik, and P. Singer, Phys. Rev. D **70,** 074022 (2004).

[33] R. Fleischer and D. Wyler, Phys. Rev. D **62,** 057503 (2000).

[34] V. V. Kiselev, O. N. Pakhomova, and V. A. Saleev, J. Phys. G **28,** 595 (2002).

[35] G. L. Castro, H. B. Mayorga, and J. H. Munoz, J. Phys. G **28,** 2241 (2002).

[36] V. A. Saleev, Phys. At. Nucl. **64,** 2027 (2001); O. N. Pakhomova and V. A. Salev, Phys. At. Nucl. **63,** 1999 (2000).

[37] Y. S. Dai and D. S. Du, Eur. Phys. J. C **9**, 557 (1999); D. S. Du and Z. T. Wei, Eur. Phys. J. C **5**, 705 (1998).

[38] M. Masetti, Phys. Lett. B **286**, 160 (1992).

[39] Q. P. Xu and A. N. Kamal, Phys. Rev. D **46**, 3836 (1992).

[40] J. Sun, Y. Yang, W. Du, and H. Ma, Phys. Rev. D **77**, 114004 (2008).

[41] M. A. Ivanov, J. G. Körner, and O. N. Pakhomova, Phys. Lett. B **555**, 189 (2003).

[42] F. Hussain and M. D. Scadron, Phys. Rev. D **30**, 1492 (1984).

[43] H.-M. Choi and C.-R. Ji, Phys. Rev. D **80**, 054016 (2009).

[44] H.-M. Choi and C.-R. Ji, Phys. Rev. D **59**, 074015 (1999).

[45] H.-M. Choi and C.-R. Ji, Phys. Lett. B **460**, 461 (1999).

[46] C.-R. Ji and H.-M. Choi, Phys. Lett. B **513**, 330 (2001).

[47] H.-M. Choi, C.-R. Ji, and L. S. Kisslinger, Phys. Rev. D **65**, 074032 (2002).

[48] H.-M. Choi, Phys. Rev. D **75**, 073016 (2007); J. Korean Phys. Soc. **53**, 1205 (2008).

[49] H.-M. Choi, Phys. Rev. D **77**, 097301 (2008).

[50] M. Bauer, B. Stech, and M. Wirbel, Z. Phys. C **34**, 103 (1987).

[51] M. Neubert and B. Stech, Adv. Ser. Dir. High Energy Phys. **15**, 294 (1998).

[52] H. Y. Cheng, Phys. Lett. B **335**, 428 (1994); L. L. Chau and H. Y. Cheng, Phys. Rev. D **36**, 137 (1987).

[53] A. Szczepaniak, E. Henley, and S. J. Brodsky, Phys. Lett. B **243**, 287 (1990).

[54] N. Deshpande, M. Gronau, and D. Sutherland, Phys. Lett. **90B**, 431 (1980); Nucl. Phys. **B183**, 367 (1981).

[55] A. N. Kamal, Phys. Rev. D **33**, 1344 (1986).

[56] J. D. Bjorken, Nucl. Phys. B, Proc. Suppl. **11**, 325 (1989).

[57] C. Amsler *et al.* (Particle Data Group), Phys. Lett. B **667**, 1 (2008).

[58] M. Beneke, G. Buchalla, M. Neubert, and C. T. Sachrajda, Phys. Rev. Lett. **83**, 1914 (1999); Nucl. Phys. **B591**, 313 (2000).

[59] A. J. Buras and L. Silvestrini, Nucl. Phys. **B569**, 3 (2000).

[60] H.-M. Choi and C.-R. Ji, Phys. Rev. D **75**, 034019 (2007).

[61] D. Scora and N. Isgur, Phys. Rev. D **52**, 2783 (1995).

[62] H.-M. Choi and C.-R. Ji, Phys. Rev. D **58**, 071901(R) (1998); **72**, 013004 (2005); S. J. Brodsky and D. S. Hwang, Nucl. Phys. **B543**, 239 (1999).

[63] W. Jaus, Phys. Rev. D **60**, 054026 (1999).

[64] T. Feldmann, P. Kroll, and B. Stech, Phys. Rev. D **58**, 114006 (1998); Phys. Lett. B **449**, 339 (1999).

[65] T. Feldmann, Int. J. Mod. Phys. A **15**, 159 (2000).

[66] H. Leutwyler, Nucl. Phys. B, Proc. Suppl. **64**, 223 (1998).

[67] S. L. Adler, Phys. Rev. **177**, 2426 (1969); J. S. Bell and R. Jackiv, Nuovo Cimento A **60**, 47 (1969); J. Gasser and H. Leutwyler, Nucl. Phys. **B250**, 465 (1985); J. F. Donoghue, B. R. Holstein, and Y. C. R. Lin, Phys. Rev. Lett. **55**, 2766 (1985).

[68] M. Artuso *et al.* (CLEO Collaboration), Phys. Rev. Lett. **95**, 251801 (2005).

[69] J. P. Alexander *et al.* (CLEO Collaboration), Phys. Rev. D **79**, 052001 (2009).

[70] K. W. Edwards *et al.* (CLEO Collaboration), Phys. Rev. Lett. **86**, 30 (2001).

[71] L. Wolfenstein, Phys. Rev. Lett. **51**, 1945 (1983).